EUROPEAN ORGANIZATION FOR NUCLEAR RESEARCH

Ce DOPED HAFNIATE SCINTILLATING GLASSES:
THERMALLY STIMULATED LUMINESCENCE
AND PHOTOLUMINESCENCE

M. Martini, F. Meinardi, A. Vedda
*INFM - Dipartimento di Fisica dell'Universita' di Milano, via Celoria 16, I20133
Milano, Italy*
I. Dafinei*, P. Lecoq
CERN, PPE Div., 1211 Geneva - 23, Switzerland
M. Nikl
Institute of Physics CAS, Cukrovarnicka 10, 162 00 Prague, Czech Republic

Abstract

Thermally stimulated luminescence (TSL) and time resolved luminescence studies have been performed on undoped, and Ce^{3+} and Mn^{2+} doped fluoro-hafniate glasses (HFG). The X-ray induced TSL glow curve above room temperature features different broad structures extending up to 350 °C; wavelength resolved measurements put in evidence the existence of two distinct emission peaks around 300 nm and 550 nm, attributed to Ce^{3+} and Mn^{2+} ions respectively. The role of Ce^{3+} and Mn^{2+} dopant ions in the trapping-recombination TSL processes was investigated, on the basis of the analysis of the spectral distribution of the emitted light at different dopant ions concentrations, and of the dose dependencies of the signals. Time resolved luminescence measurements allowed a detailed characterization of both Ce^{3+} and Mn^{2+} emissions. Their decay times were found to be 19.2 ns and 27 ms, respectively; the excitation spectrum of the 550 nm emission revealed the existence of a radiative energy transfer between Ce^{3+} and Mn^{2+} centers, while non radiative transfer processes were not observed.

---

*) On leave from IFA, Bucharest, Romania

1. Introduction

In recent years there has been a growing effort on the study of the optical properties of CeF_3, due to a great interest in high density, fast, and radiation hard Ce-doped scintillators for high energy physics and medical applications [1].

Photoluminescence and scintillation studies, performed on pure CeF_3 and on mixed cerium lantanum trifluoride ($Ce_xLa_{1-x}F_3$), established that the parity allowed transitions from 5d to splitted 4f levels of Ce^{3+} ions are responsible for the observed emissions at 286 nm and at 305 nm [2]. A third emission, observed at 340 nm and whose intensity appears to be strongly dependent upon the growth conditions and purity of the crystal, was ascribed to the same transition occurring at "perturbed" cerium ions, possibly located in the proximity of fluorine vacancies [2]. Time resolved spectroscopy studies revealed the existence of both radiative and non-radiative energy transfer processes from "regular" to "perturbed" cerium sites [3, 4].

Glasses have also been considered as host materials for Ce activators [5,6] in alternative to crystals, the main advantage of scintillating glasses being that they present large possibilities for compositional improvements. However, their optical properties were less investigated: recent studies on the scintillation properties of various classes of heavy fluoride glasses (fluoro-aluminates, fluoro-hafniates and fluoro-zirconates) with different CeF_3 concentrations [6,7] demonstrated that they are characterized by a relatively low light yield, possibly due to the presence of charge traps reducing the efficiency of charge transport to Ce^{3+} ions; the radiation hardness of these materials was found to be lower than that of CeF_3 crystals, even if it could be compensated by optical and thermal bleaching treatments. Fortunately, in hafnium fluoride glasses these effects were weaker with respect to other glasses, and the results encouraged the interest toward a deeper investigation of the optical properties of these materials. Manganese doping was found to increase light yield [5], but with this respect controversial results were also obtained [7].

It is the aim of this work to study both the thermoluminescence and photoluminescence properties of the above mentioned hafnium fluoride glasses with different cerium concentrations: time resolved photoluminescence measurements have allowed to determine the optically excited properties of Ce^{3+} in the amorphous matrix, and to compare them with the well understood mechanisms operating in CeF_3 and $Ce_xLa_{1-x}F_3$ crystals, while the thermoluminescence measurements have given a deeper insight in the investigation of charge traps affecting the light output and scintillation efficiency. The relevant effects, both on thermo- and photoluminescence, of the incorporation of Mn^{2+} ions in the host have also been considered.

2. Experimental conditions

2

The glasses studied in this work were heavy hafnium fluoride glasses (HFG) produced by the company "Le Verre Fluoré", France, with density of 5.95 g/cm^3. Samples with different concentrations of Ce (up to 10%) and of Mn (up to 2%) were considered. In the following, samples will be denoted as HFG(x,y), where x and y represent the Ce and Mn percentage concentrations, respectively. For nominally undoped samples, in which however cerium and/or manganese are present as impurities at concentrations lower than 0.01%, x=0, y=0 will be indicated.

Emission, excitation spectra and photoluminescence decay were measured using a Spectrofluorimeter 199S manufactured by Edinburgh Instrument. As excitation sources, a hydrogen steady-state flashlamp was used for steady-state measurements, a hydrogen filled coaxial flashlamp (nsec pulses) and a xenon flashlamp (µsec pulses) were used for the decay measurements. Emission and excitation spectra were corrected for spectral response of the detection part and spectral energy dependence of the excitation part, respectively. For ns decays, deconvolution procedure was used to extract true decay times.

TSL measurements were performed from room temperature up to 350°C with a linear heating rate of 0.5 °C/s by means of two different apparatuses: in the first the total emitted light was detected as a function of temperature by the technique of photon counting using an EMI 9635 QB photomultiplier tube. The second consisted of a home made high sensitivity spectrometer measuring wavelength resolved TSL [8].

The samples were irradiated at room temperature with a X-ray tube (Machlett OEG 50, tungsten target) operating at 30 kV, and the dose values ranged from 10^1 Gy up to 5×10^4 Gy.

3. Results

3a. Photoluminescence

Emission properties of HFG(Ce,Mn) samples are given in Fig. 1. Nominally undoped HFG(0,0) shows characteristics Ce^{3+} emission peaking at 295 nm. Highly Ce^{3+} doped HFG(2.5,0) and HFG(5,2) samples show "the shift" of emission to longer wavelength side, which is at least partly given by selfabsorption at Ce^{3+} sites, phenomenon well known e.g. in CeF_3 [9]. In sample HFG(5,2), codoped by 2% of Mn^{2+}, emission at about 550 nm is observed with decay time about of 27 ms at 295 K, which are parameters characteristics for Mn^{2+} centres. The inset of the figure shows the 19.2 ns decay time of Ce^{3+} emission of nominally undoped HFG(0,0) sample. This value perfectly matches the values observed in LaF_3:Ce or CeF_3. We note that the Ce^{3+} decay time is not shortened in manganese codoped HFG(5,2) (22 ns), and that there is also good agreement with the HFG(2.5,0) Ce^{3+} decay time (round 21 ns). When excited at

about 250 nm and collecting the emission from the side of the sample, distinct influence of the re-absorption of Ce^{3+} emission is observed - decay time becomes longer - about 28-29 ns.
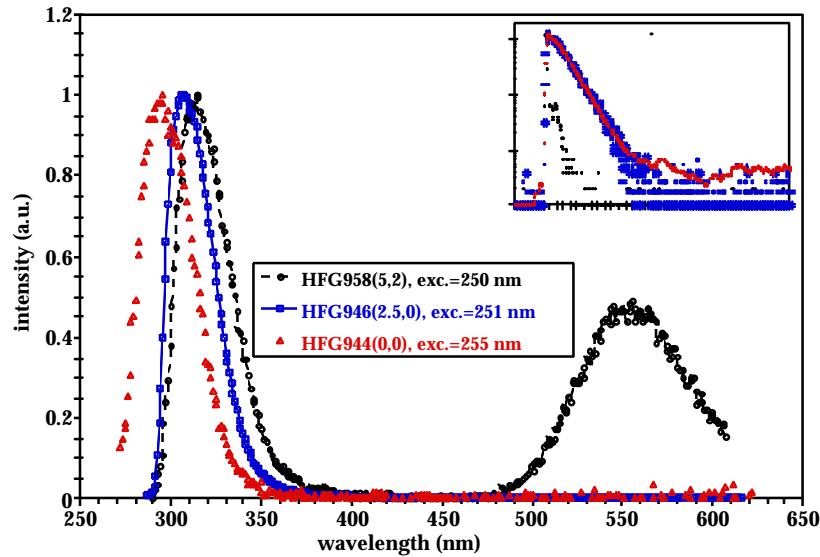

Fig.1 Emission spectra of HFG glasses at room temperature. Numbers in the parentheses in the legend indicate weight percent concentrations of Ce and Mn, respectively. The wavelength of excitation is given as well. The photoluminescence decay curve of HFG 944(0,0) sample (T=295 K, exc.=255 nm, em.=300 nm) is given in the inset. The solid line is the convolution of the instrumental response and a single exponential with the decay time τ=19.2 ns.
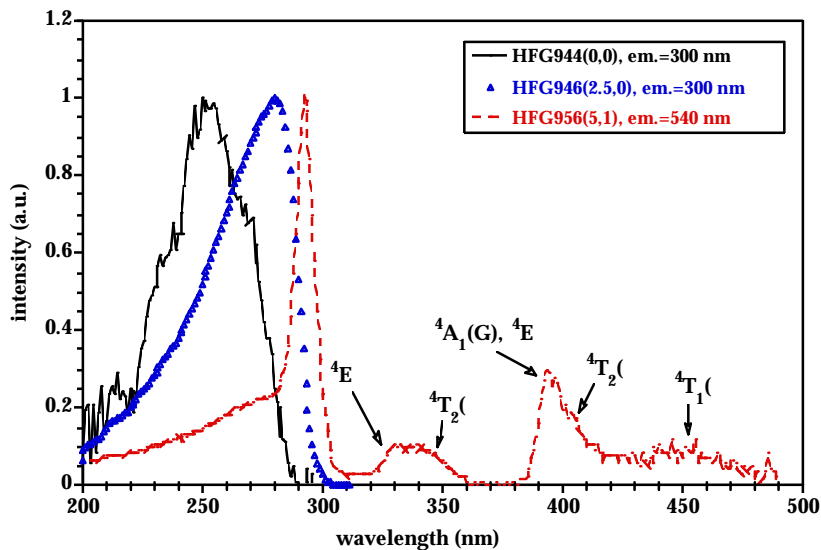

Fig.2: Excitation spectra of HFG glasses at room temperature. The wavelength of emission is given in the legend. The symbols indicate the Mn^{2+} excited state levels involved in the transitions from the $6A_1$ ground state of Mn^{2+} ions.

Excitation spectra, shown in Fig. 2, show dominant Ce^{3+} excitation below 300 nm, and for HFG(0,0) even splitting of excited 5d states can be observed. As

for Mn^{2+} excitation, transitions above 300 nm can be ascribed to the Mn^{2+} (isolated or Suzuki phase) centres (cubic environment approximation) using results obtained e.g. for NaCl:Mn [10]. The shape of Mn^{2+} excitation spectrum below 300 nm is mostly given by the fact that Ce^{3+} emission is efficiently excited in this region and reabsorbed by Mn^{2+} absorption bands in 320-350 nm region. Sharp peak round 290 nm is probably partly given just by "geometrical factor" - sudden increase of excited volume of the sample because of the drop of Ce^{3+} absorption in this region. However, contribution of Mn^{2+} transition $6A_1$-$4T_1$(P) is not excluded.

3b. Thermally Stimulated Luminescence (TSL)

Fig. 3 shows the X-ray induced TSL glow curves above room temperature of three HFG glasses, characterized by different cerium and manganese concentrations: curve a) is relative to HFG(5,2), while curves b) and c) are relative to HFG(10,2) and HFG(5,1), respectively. In all cases, a broad
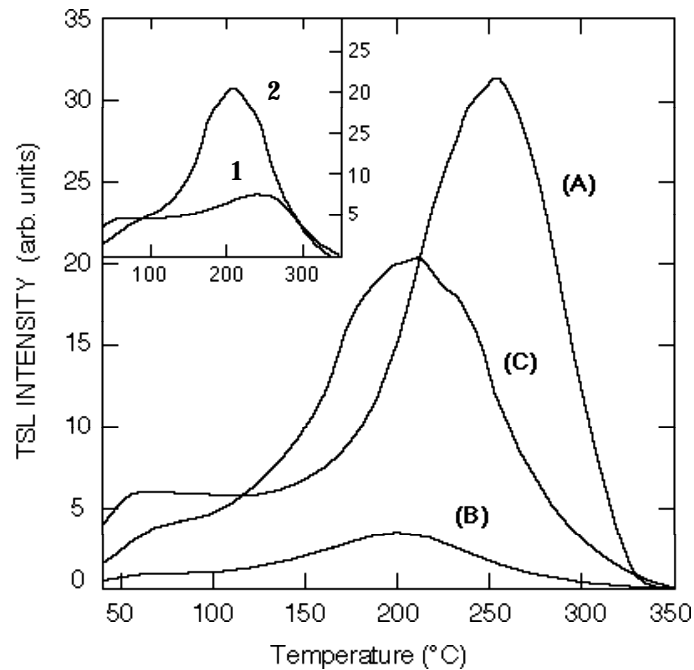

Fig.3: TSL glow curves induced by a 2.5x103 Gy X-ray irradiation on various heavy fluoride glasses characterized by different cerium and manganese concentrations. (A), 5%Ce and 2%Mn (HFG(5,2)); (B), 10%Ce and 2%Mn (HFG(10,2)); (C), 5%Ce and 1%Mn (HFG(5,1)). The inset shows the comparison between the first TSL measurement (curve 1) and successive runs (curve 2) on HFG(5,1).

and unresolved signal extending up to 350 °C is observed: the increase of manganese dopant is responsible for a signal enhancement and for a shift of the glow curve maximum toward higher temperatures. On the contrary, a marked reduction of the glow curve intensity is evidenced by increasing cerium concentration. Besides signal reduction, a shift of the glow curve maximum

toward lower temperatures is also observed with increasing cerium concentration. These measurements were taken after the samples were subjected to a first heating cycle up to 350 °C, when a good reproducibility of the signals with respect to successive runs was observed. The effect of a first heating cycle up to 350 °C is displayed in the inset of the figure, which shows the comparison between the first glow curve obtained on HFG(5,1) (curve 1) and one of the successive measurements (curve 2): it appears that the first heating cicle is effective in enhancing the TSL sensitivity. This effect was found in all the samples that we analyzed, with similar characteristics.

The wavelength distribution of the TSL signals was also investigated. In Fig. 4 is reported a contour plot of a measurement performed on the HFG(2.5,0) sample. Two bands are present: the weaker, due to the emission of Ce^{3+} ions, is centred at 308 nm (4.02 eV); the other, centred at 552 nm, (2.25 eV), is a typical feature of Mn^{2+} ions, present as inadvertent contamination in nominally Mn-free samples. Black body emission is also evidenced at higher wavelengths. We found that the emission at 552 nm dominates the spectrum in all samples, except in heavily Ce doped HFG(10,0), and becomes very strong in intentionally manganese doped samples, where the Ce band is no longer observed. In the nominally undoped sample, another very weak band at 390 nm was also detected: for this emission, a host matrix related nature can be suggested, however a precise attribution is lacking.

The glow curves of the two emissions are not the same: the 308 nm band peaks at approximately 225 °C, while the 552 nm band is peaked at approximately 170 °C.
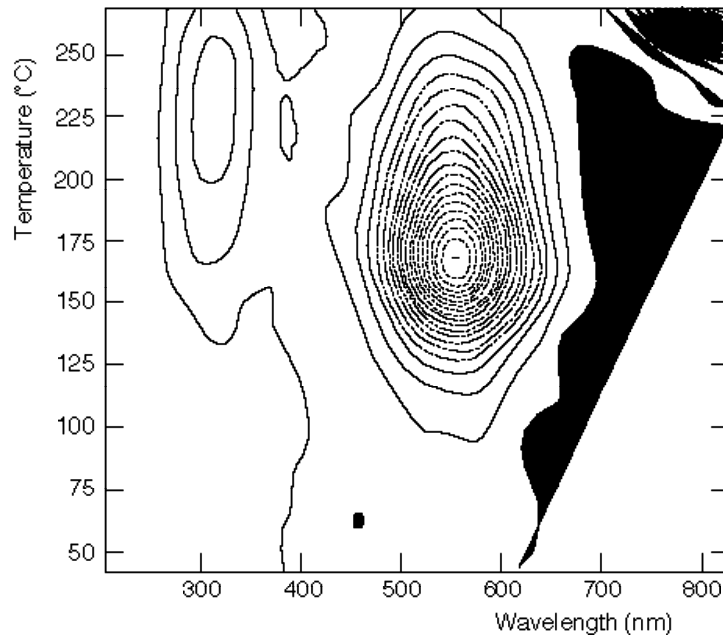

Fig.4: Wavelength resolved TSL measurement performed on a HFG(2.5,0) sample. The X-ray dose was 5×10^4 Gy.
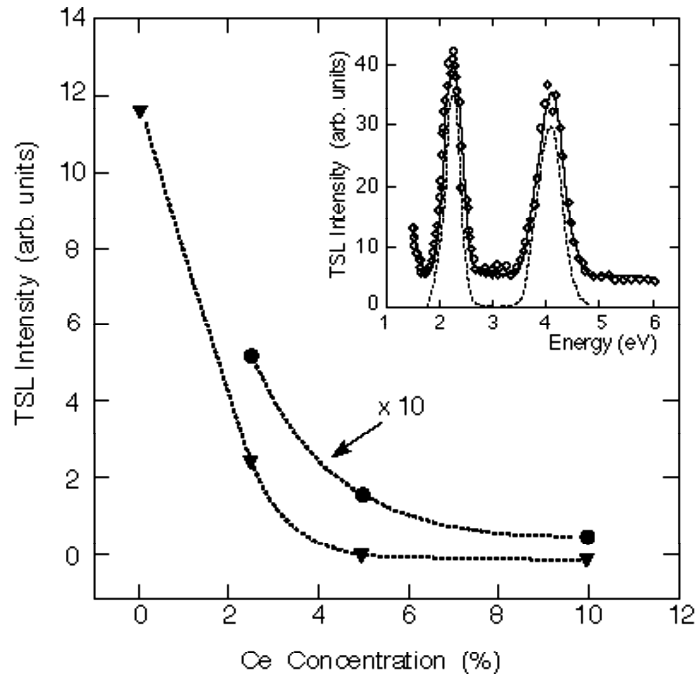
6

Fig.5: Intensities of the TSL bands as a function of cerium dopant concentration for a 5x104 Gy x-ray irradiation dose. Circles, "300 nm" band; triangles, "552 nm" band. Samples were nominally free of manganese dopant. The inset shows the energy spectrum of the TSL, with deconvolution into gaussian components. Circles, experimental data; full line, calculated spectrum; dashed line, gaussian components. Integration has been performed in the 200-300 C region, in which the intensities of the two bands are similar.
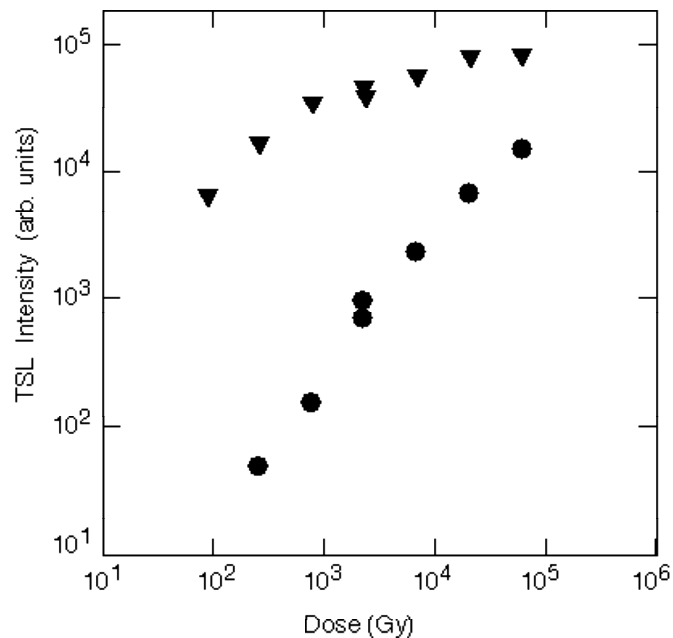

Fig.6: TSL intensities versus dose of two different samples. Triangles, HFG(0,0); circles, HFG(2.5,0). Reported signals are integrated intensities, as detected by EMI 9635 photomultiplier tube. Two different dose rates were used in order to cover the complete range: open symbols, 500 Gy/min; filled symbols, 5000 Gy/min.

In order to investigate the role of cerium dopant in the TSL emissions, we considered nominally Mn free samples characterized by different cerium concentrations. The intensities of the two emissions are displayed in Fig. 5 versus cerium concentration: a strong quenching of both emissions, and particularly of that relative to manganese present as inadvert impurity, is observed. In the inset is shown the energy spectrum of the TSL intensity of a HFG (2.5,0) sample integrated from 200°C to 300°C (temperature range where the intensities of the two emissions are of the same order of magnitude), together with a fit into gaussian components. For the manganese emission, the gaussian fit led to E=2.24 eV, FWHM=0.36 eV. In accordance with photoluminescence results, we also observed that the Ce emission is shifted toward lower energies with increasing cerium concentration: for the HFG(2.5,0) E=4.02 eV, FWHM=0.54 eV parameters were found.

The effect of cerium doping was also investigated from the point of view of the dose dependence of the TSL signal, in the dose range from $5x10^1$ to $5x10^4$ Gy. Fig. 6 gives the integrated intensities of the TSL signal as detected by EMI9635 photomultiplier tube for a nominally undoped HFG(0,0) and a HFG(2.5,0) sample. The undoped sample shows a saturating behaviour above $5x10^2$ Gy, while the cerium doped specimen features good linearity of the intensity versus dose in the whole range considered.

4. Discussion and Conclusions

The observed optical emission-excitation features allow a comparison with the already studied properties of crystalline cerium compounds. The Ce^{3+} emission in HFG matrix is similar to what is observed in LaF_3:Ce and CeF_3 single crystal matrices. Spectral shapes are smoothed by the influence of the glass host, while the decay times are nearly the same as e.g. in CeF_3 (the transition dipole matrix element is not changed by the change from crystalline to glass matrix, as the site symmetry in both cases is very low). The lengthening of Ce^{3+} decay time because of reabsorption is probably higher than in crystalline hosts, because of extended distribution of non-equivalent sites in glass host.

Mn^{2+}-codoping doesn't lead to enhanced "perturbed-Ce^{3+}" emission in the region 340-360 nm as observed for Ba^{2+}-doped CeF_3 [3]. This might be again explained by the glass character of the host matrix, which probably does not require the creation of an anion charge balancing the vacancy next to Mn^{2+} ions. This vacancy was recognized as the key defect in CeF_3 structure responsible for perturbed Ce-sites and emission in 340-360 nm region.

Taking into account the spectral overlap between Ce^{3+} emission and Mn^{2+} excitation bands in the 320-350 nm region, one can explain the Ce^{3+}-Mn^{2+} energy transfer observed. The fact that the decay time of Ce^{3+} emission is not affected by Mn^{2+} codoping, proves that the energy transfer is mostly only the radiative one and no efficient nonradiative energy transfer paths are available. In

the latter case, increasing decay non-exponentiality and shortening of the mean donor decay time would be noticed, as observed e.g. in KCl:Eu^{2+}, Mn^{2+} system [11].

The TSL results have given a deeper insight in the knowledge of charge traps, possibly affecting the scintillation efficiency of the material. TSL glow curves are characterized by broad and unresolved structures, extending in the whole temperature range considered: this calls for the presence of a complex distribution of trap depths, as can be expected in an amorphous and composite host matrix [12,13]. The observed slight TSL sensitivity increase after a first heating cycle up to 350 °C can be tentatively ascribed to the presence, in untreated samples, of CeF$_3$ aggregates, where non-radiative recombinations between free electrons and holes take place. The thermal treatment could promote a partial dissolution of these CeF$_3$ aggregates, thus reducing the probability of non radiative recombinations.

The shift of the maximum of the glow curve toward higher temperatures, and the higher TSL intensity observed in Mn doped samples suggest that this dopant ion (present also as inadvertent contamination in nominally undoped samples) is responsible for the introduction of additional deeper traps, even if the available data do not allow to propose specific attributions for such defects. Moreover, the temperature difference between the maxima of the two emissions at 308 and 552 nm, evidenced in Fig. 4, suggests the presence of a spatial correlation between traps and luminescent centres. Manganese is also much more efficient, with respect to cerium, as recombination centre: in fact, the 552 nm emission dominates the TSL spectrum of intentionally Mn-doped samples, even in the presence of higher cerium concentrations.

The most important role of cerium dopant ions evidenced by the present TSL results is that of a strong quenching of the signal intensity. In this regard, different mechanisms can be suggested, possibly simultaneously operating in this situation. Processes competitive with respect to the TSL trapping-recombination phenomena can be present: during irradiation, cerium ions could compete in carrier capture with shallow traps responsible for thermoluminescence; moreover, high cerium concentrations could be responsible for a significant probability of non radiative transitions during the phase, thus giving rise to lower TSL signals. Alternatively, the presence of this dopant could partially prevent the formation of point defects which provide trap levels. To this point, we remind that it is well known that cerium has the ability to enhance the radiation hardness of a host matrix: in fact, Ce^{3+}, by loosing its 4f electron, prevents the formation of V-centre like defects; similarly, by capturing ionized electrons which would be trapped by anion vacancies, Ce^{4+} can prevent the formation of F-centre like defects [6]. The different shapes of the glow curves, and different dependencies of the signal intensities upon X-ray dose observed in undoped and cerium doped samples support the existence of this second quenching mechanism.

References

1.D.F. Anderson, IEEE Trans. Nucl. Sci. 36, 137 (1989).

2.C. Pedrini, B. Moine, J.C. Gacon and B. Jacquier, J. Phys. Cond. Matter 4, 5461 (1992).

3.M. Nikl, C. Pedrini, Sol. St. Comm. 90, 155 (1994).

4.A. J. Wojtowicz, M. Balcerzyk, E. Berman and A. Lempicki, Phys. Rev. B 49, 14880 (1992).

5.E.G. Devitsin, L.N. Dmitruk, V.A. Kozlov, A.A. Komar, M.I. Kotov, L.S. Popov, S.Yu. Potashov, "Heavy Scintillators for Scientific and Industrial Applications", Proc. of the "Cristal 2000" International Workshop, Sept. 22-26, 1992, Chamonix, France, Ed. FrontiËres, p. 401-406.

6.M.J. Weber, "Heavy Scintillators for Scientific and Industrial Applications", Proc. of the "Cristal 2000" International Workshop, Sept. 22-26, 1992, Chamonix, France, Ed. FrontiËres, p. 99-124.

7.I. Dafinei, E. Auffray, P. Lecoq, M. Schneegans, Mat. Res. Soc. Symp. Proc. 348, "Scintillators and Phosphor materials" April 6-8, 1994, San Francisco, California, USA, p. 217-221.

8. M.Martini, S.Paravisi and C. Liguori, Radiation Measurements, to be published.

9.S. Anderson et al, Nuclear Instruments and Methods in Phys. Res. A332, 373 (1993).

10.F. Rodriguez, M. Moreno, F. Jaque and F.J. Lopez, J. Chem. Phys. 78, 73 (1983).

11.R. Capelletti, M. Manfredi, R. Cywinski, J. Z. Damm, E. Mugenski, M. Solzi, Phys. Rev. B 36, 5124 (1987).

12.A.R. Spowart, J. Phys. C: Solid State Phys. 12, 3369 (1979).

13.M. Martini, G. Spinolo, A. Vedda, C. Arena, Solid State Commun. 91, 751 (1994).